

## Supporting information

### Synthesis, Crystal Structure and Study of Magnetocaloric Effect and Single Molecular Magnetic Behaviour in Discrete Lanthanide Complexes

Amit Adhikary, Javeed Ahmad Sheikh, Soumava Biswas and Sanjit Konar\*

Department of Chemistry, IISER Bhopal, Bhopal- 462066, India, Fax: (+91) 7556692392.

**Table S1. Selected hydrogen bonding distances ( $\text{\AA}$ ) and angles (deg) for the complex 1**

D-H....A	Symmetry operation	D-H( $\text{\AA}$ )	A...H( $\text{\AA}$ )	D....A( $\text{\AA}$ )	$\angle$ D-H-A(deg)
C7-H7....O2	x,y,z	0.930	2.607	3.179	120
O1-H1A-...Cl2	x,y,z	0.851	2.258	2.934	136
O9-H9A-...Cl2	x,y,z	0.850	2.154	2.845	138
O3-H3A-...Cl3	-x,+y,-z+1/2 +1	0.850	2.631	3.202	126
O11-H11A...N3	-x,-y+1,-z+1	0.930	2.355	2.881	120

**Table S2. Selected hydrogen bonding distances ( $\text{\AA}$ ) and angles (deg) for the complex 2**

D-H....A	Symmetry operation	D-H( $\text{\AA}$ )	A...H( $\text{\AA}$ )	D....A( $\text{\AA}$ )	$\angle$ D-H-A(deg)
O21- H21B...Cl3	x,y,z	0.901	2.319	3.077	141
O9 -H9A ...O6	x,y,z	0.880	2.157	2.776	129
C18-H18...O10	x,y,z	0.930	2.576	3.158	121
O3w-H3wA...Cl2	x,y,z	0.850	2.517	3.057	122
O1-H1B...Cl5	x-1,+y,+z	0.873	2.314	3.012	137
C30-H30...O10	-x,-y,-z+1	0.930	2.649	3.261	124

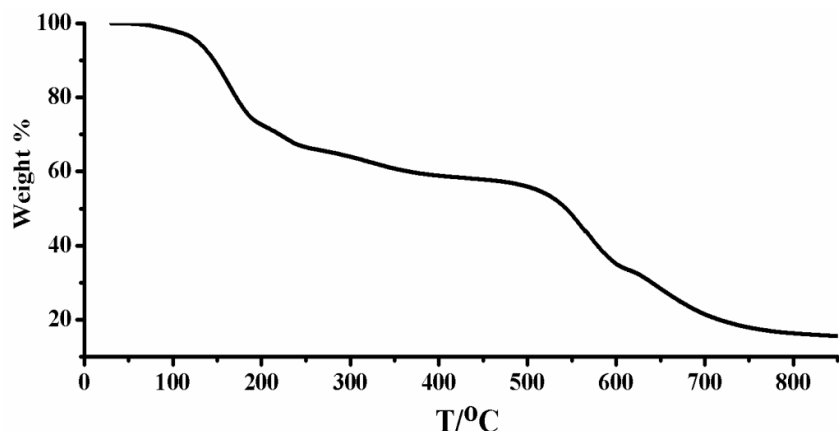


**Fig. S1.** Thermogravimetric analysis plot for complex **1**.

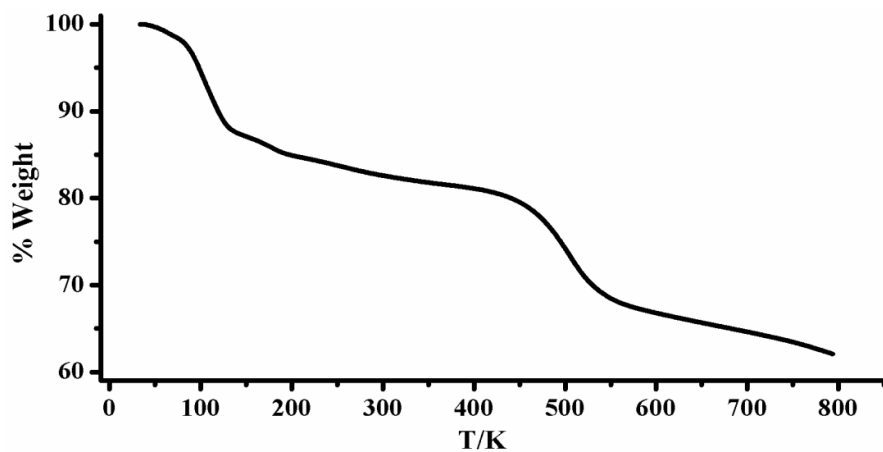


**Fig. S2.** Thermogravimetric analysis plot for complex **2**.

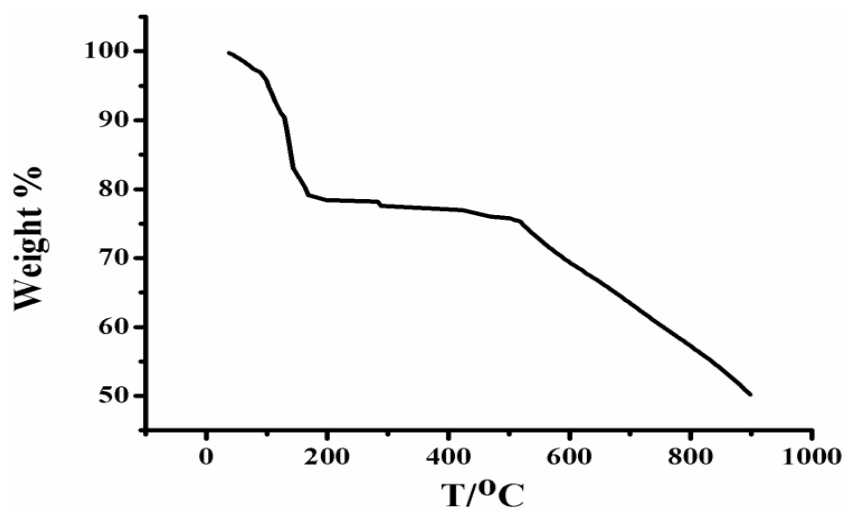


**Fig. S3.** Thermogravimetric analysis plot for complex **3**.

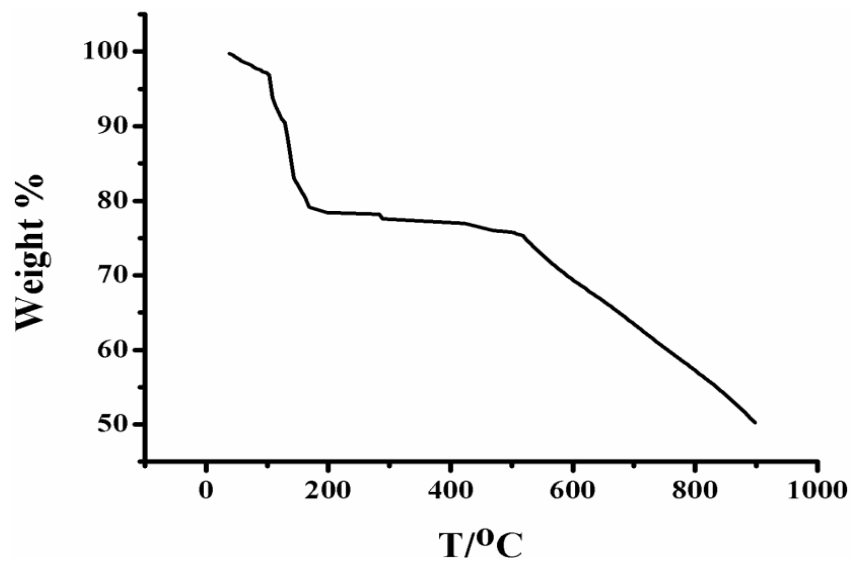


**Fig. S4.** Thermogravimetric analysis plot for complex **4**.

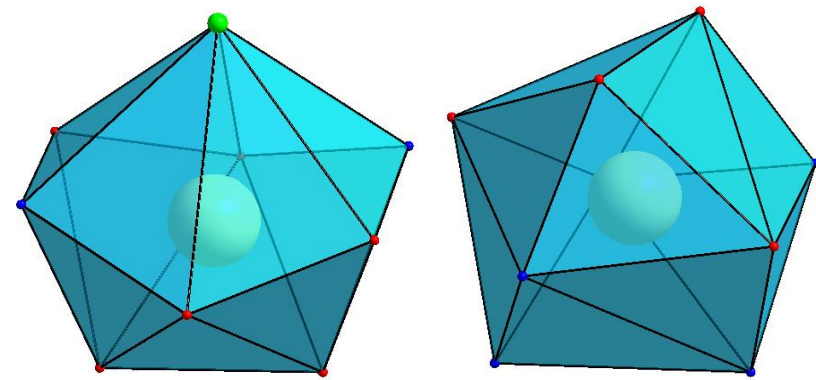


**Fig. S5.** Tri-capped trigonal prismatic geometry around  $\text{Gd}^{3+}$  with  $\text{N}_2\text{O}_6\text{Cl}$  coordination (left) and  $\text{N}_4\text{O}_5$  coordination (right) in complex **1**.

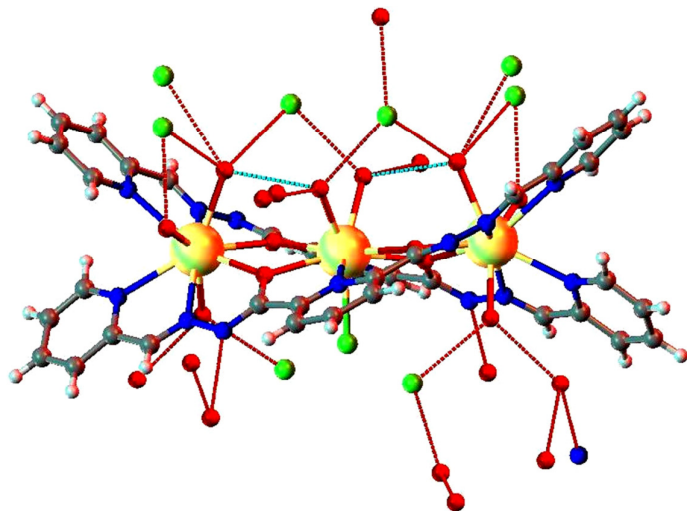


**Fig. S6.** Intra-molecular H-bonding of complex **1**

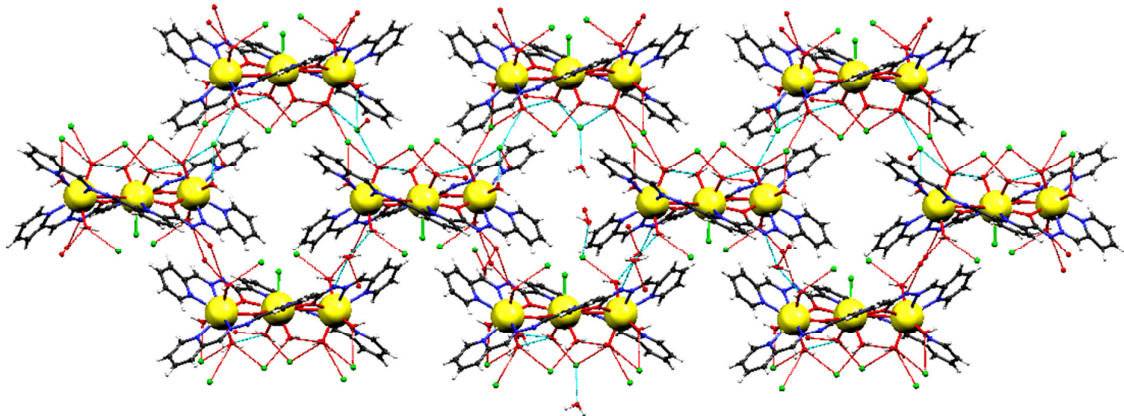


**Fig. S7.** Inter-molecular H-bonding of complex **1** along a-axis

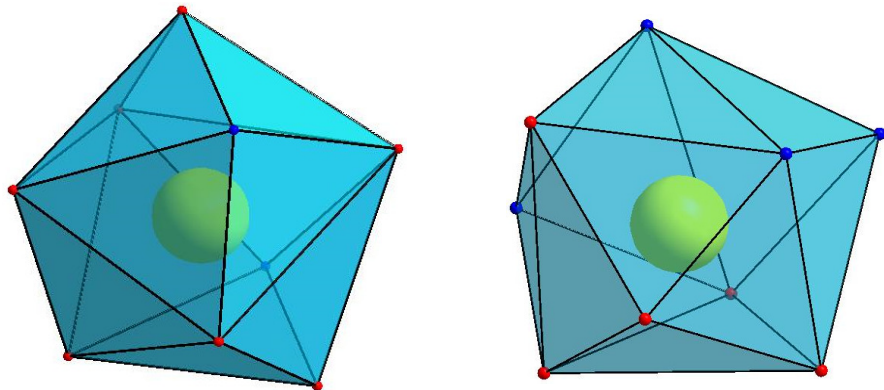


**Fig. S8.** Tri-capped trigonal prismatic geometry around Dy<sup>3+</sup> with N<sub>2</sub>O<sub>7</sub> (left) and N<sub>4</sub>O<sub>5</sub> coordination (right) in complex **2**.

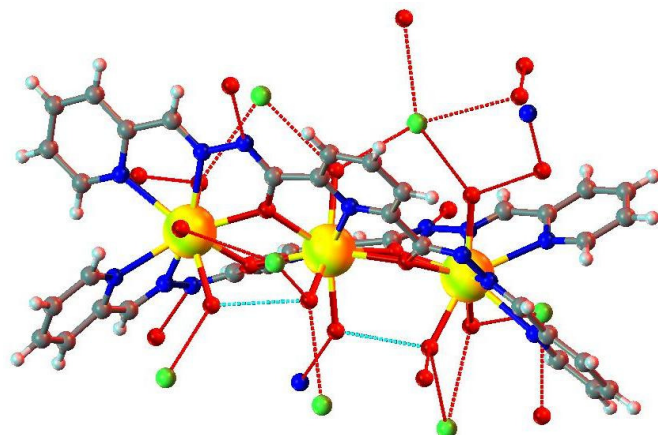


**Fig. S9.** Intra-molecular H-bonding of complex **2**

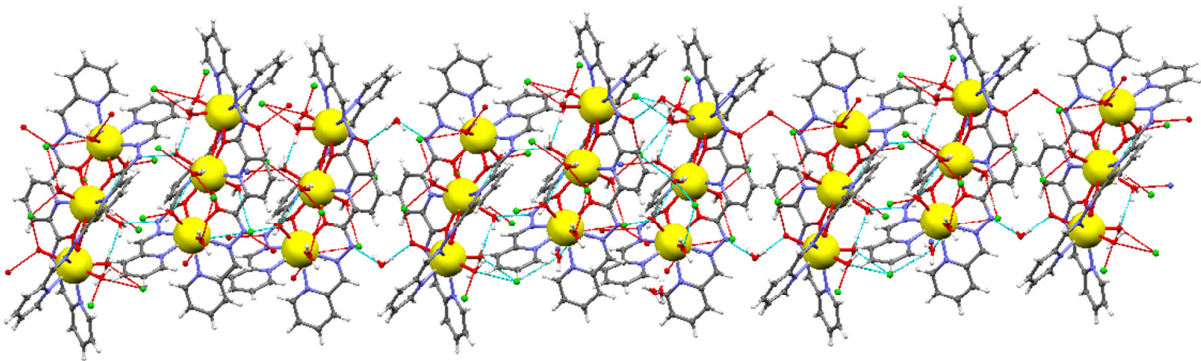


**Fig. S10.** Inter-molecular H-bonding of complex **2** along a-axis.

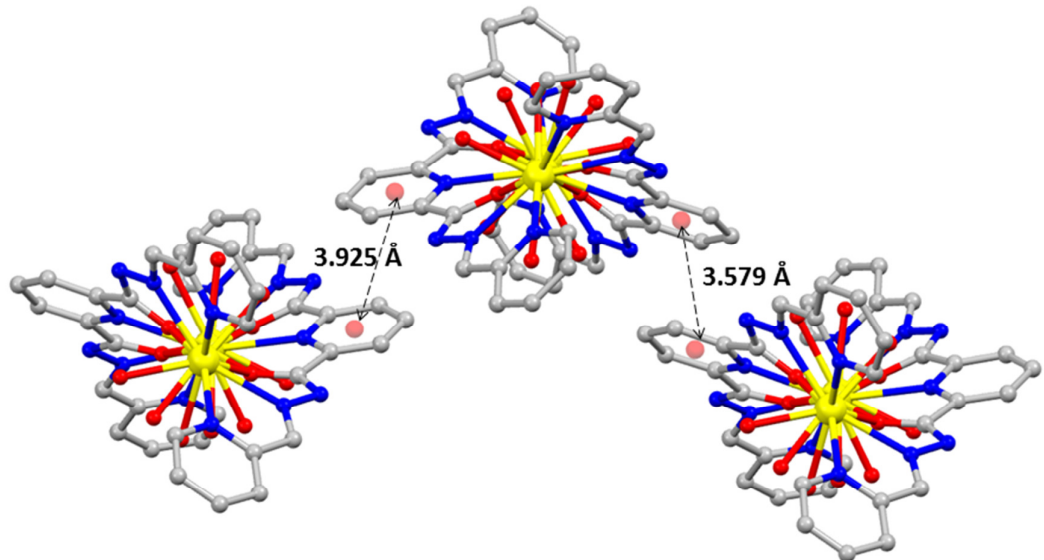


**Fig. S11.**  $\pi$ - $\pi$  stacking between pyridine ring of complex **2**.

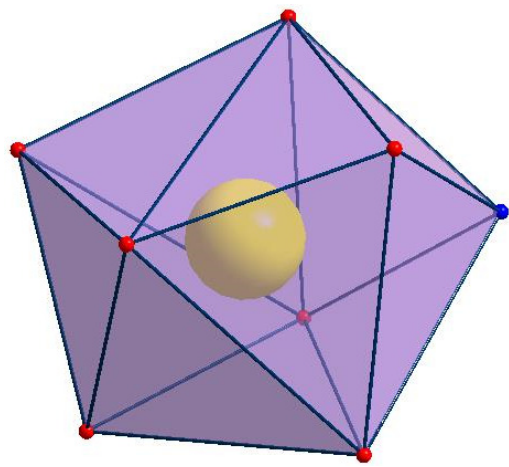


**Fig. S12.** Square antiprismatic geometry around  $\text{Ln}^{3+}$  ( $\text{Ln}^{3+} = \text{Gd}^{3+}, \text{Dy}^{3+}$ ) in complexes **3** and **4**.

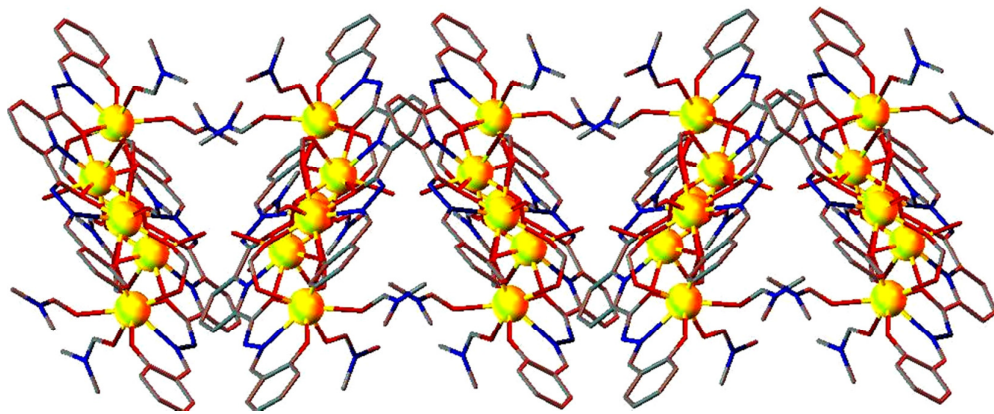


**Fig. S13.** Packing diagram of complex **3** (isostrcural complex **4**) showing zig-zag like arrangement along c-axis.

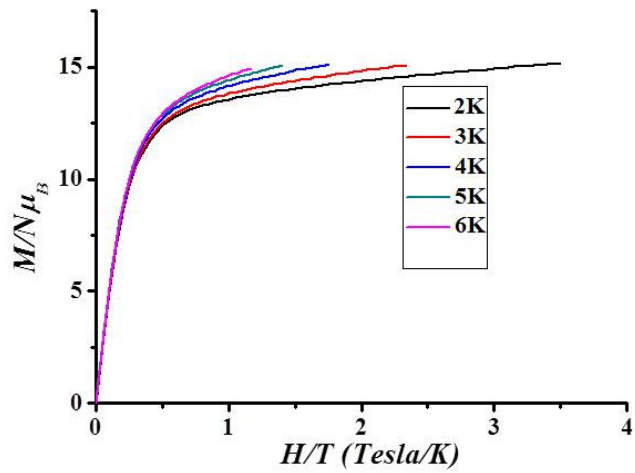


**Fig. S14.**  $M/N\mu_B$  vs  $H/T$  plots for complex **2** at 2-6 K.

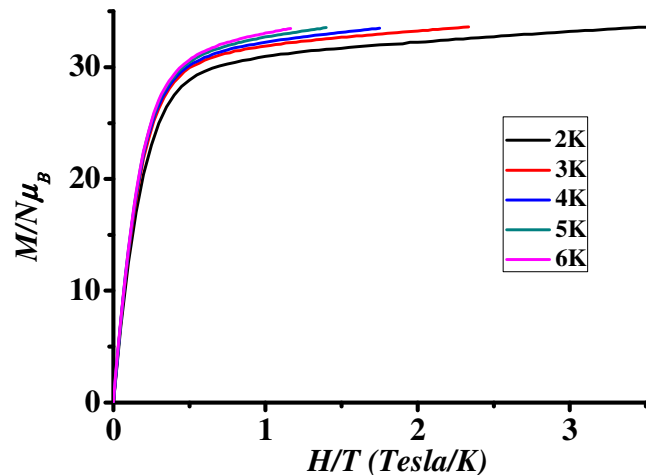


**Fig. S15.**  $M/N\mu_B$  vs  $H/T$  plots for complex **4** from 2-6 K.

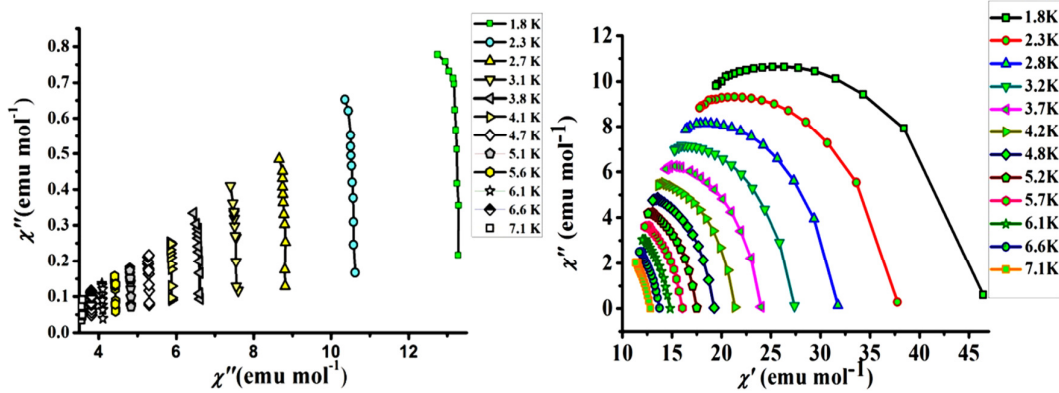


**Fig. S16.** Cole–Cole plots for complex **2** (left) and **4** (right) using the ac susceptibility data at zero field. The solid lines are to guide the eye.

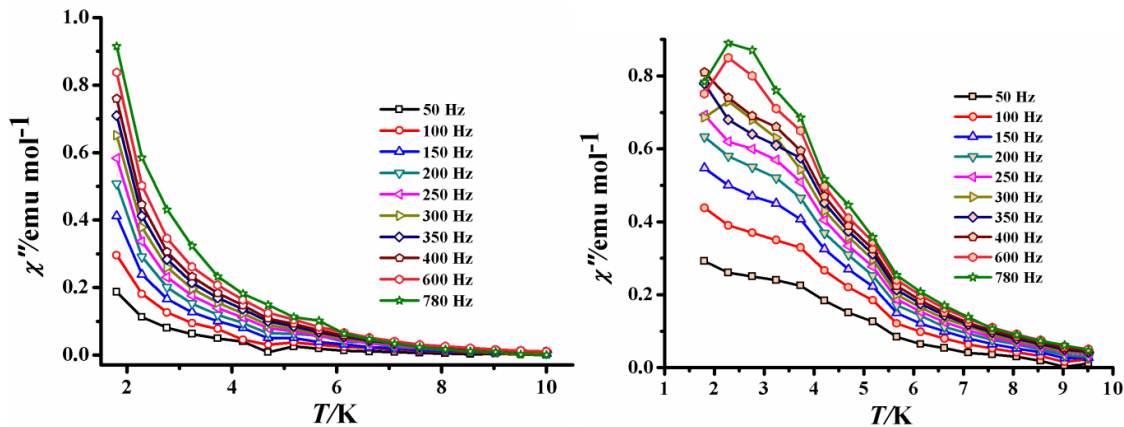


**Fig. S17.** Frequency dependence of the out of phase ( $\chi''$ ) ac susceptibility for complex **2** under a field of 1200 Oe (left) and 1600 Oe (right).

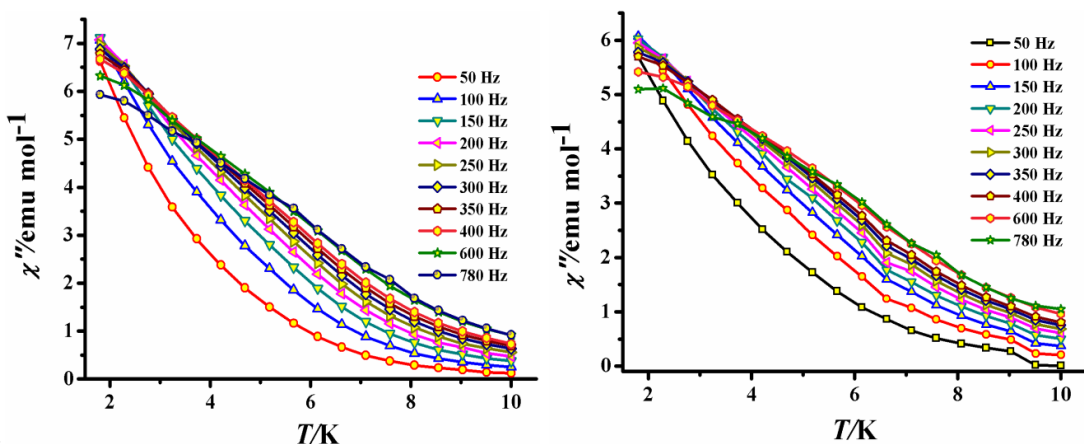


**Fig. S18.** Frequency dependence of the out of phase ( $\chi''$ ) ac susceptibility for complex **4** under a field of 1400 Oe (left) and 1600 Oe (right).

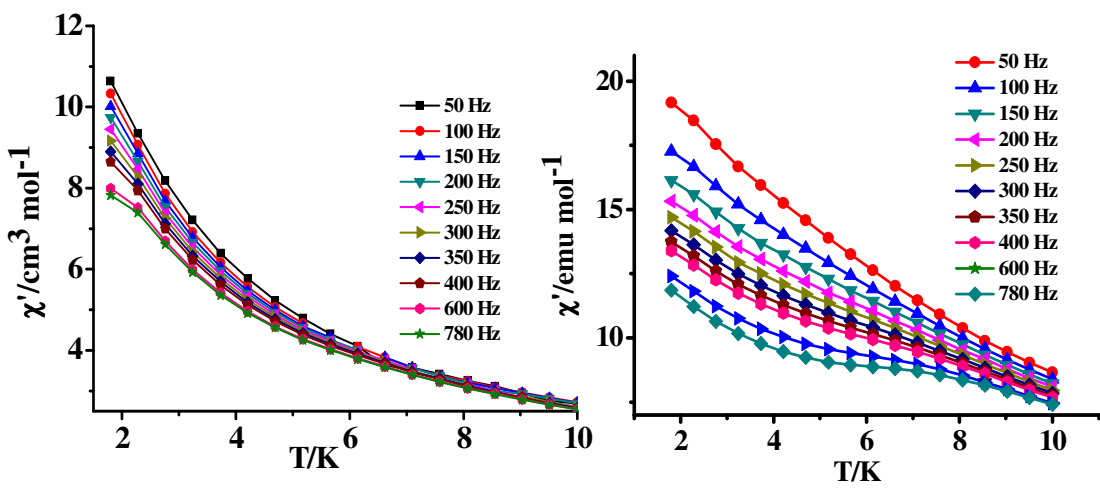


**Fig. S19.** Frequency dependence of the in phase ( $\chi'$ ) ac susceptibility for complex **2** (left) and complex **4** (right) under optimized dc fields.